NUMERICAL SIMULATION INVESTIGATION IN BEHAVIOR OF AL-FOAMS STRUCTURE UNDER HYPERVELOCITY IMPACT

Z.T. Ma, B. Jia, B.J. Pang, Y. Ha

Hypervelocity impact research center, Harbin institute of technology,
P. O. Box 3020, Science Park, Harbin Institute of Technology, Harbin, 150080, P. R. China,
Email: qw_kerry@yahoo.com.cn

ABSTRACT

The existing Equation of State and Strength Model, which regard foams as homogeneous medium, can't exactly describe the characterizations of metallic foams because the pore is big enough not to be ignored compared with projectile or bumper. In the article, Foams were regarded as discontinuous medium and pores of different size and position, fitted to some distribution and filled with void, were created in the metal to model the real geometry. Naturally material parameters needed for metallic foams are just those of original metal material, which have been developed extensively and successfully. A 3-dimansional Smoothed Particle Hydrodynamics (SPH) program with the foam model was developed. Simulations of normal impact on double bumpers, consisting of aluminum bumper and open-cell aluminum foam bumper, and aluminum rear wall were carried out and compared with test data. Good agreement was obtained. Then, the behavior of different Al-foams was investigated by numerical simulations.

1. INTRODUCTION

Tests have identified that metallic foams have a good shielding performance against M/OD hypervelocity impact, so metallic foams may play a key role in the structural design of manned spacecraft and satellite in the future (Thoma K., 2004). The evolution of the space debris population is of key interest for assessing the risk to spacecraft. Constraints for the additional weight of protection are strong in all applications, so it is necessary to achieve a higher protection efficiency and weight savings.

The behavior of metallic foams structures has strong dependence upon density, pore size and it's homogeneity, which can be changed during procedure in production or by different manufacturing techniques (Hans-Peter Degischer, 2002), so optimization of the three parameters can be done to make M/OD shield structure lighter.

SPH is a technique for problem solving in Computational Continuum Dynamics (CCD) (Randles P.W., 1996). Recently, SPH has become widely recognized for numerical simulation of hypervelocity impact. But the existing commercial computing software can't simulate foams against hypervelocity impact, for they have no appropriate foam model. And the existing Equation of State and Strength Model, which regard foams as homogeneous medium, can't exactly describe the characterizations of metallic foams, because the pore size is big enough not to be ignored compared with projectile diameter or bumper width.

2. BACKGROUND OF PROCESSING

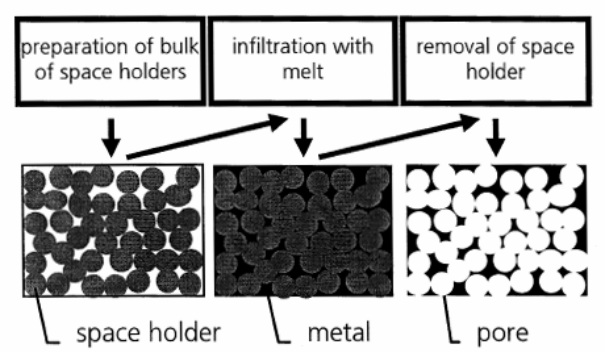

Figure 1. Production of cellular metallic materials using space-holding fillers.

Light-weight foam metals can be produced by casting liquid metal around inorganic or even organic granules or hollow spheres of low density, or by introducing such materials into a metallic melt. The granules either remain in the metallic product after casting — yielding what is called a ''syntactic foam'' — or are removed by leaching in suitable solvents or acids or by thermal treatment (see Fig. 1). This can be done successfully if the content of space holding fillers is so high that all the granules are interconnected. Vermiculite or fired clay pellets, soluble salts, loose bulks of expanded clay granules, sand pellets, foamed glass spheres or aluminum oxide hollow spheres can serve as inorganic filler material. Polymer spheres can be used as organic space holders if the solidification of the melt is sufficiently fast. The latter requires high pressure infiltration, e.g., in a die-casting machine (John Banhart, 2001).

Aluminum foams are produced by infiltration of porous salt patterns and subsequent dissolution of the salt as outlined in Fig. 2 (Marchi C. San, 1999). The pattern is

prepared by sintering a packed bed of coarse chemical grade sodium chloride powder. The particles of this high-purity salt are about 500 μm in diameter, and their shape is equiaxed, varying somewhat from cubic to spherical depending on the as-received lot (Marchi C. San, 2001).

To produce the pattern, loose salt powder is poured into alumina crucibles that have been coated with boron nitride. The crucible is then tapped until a stable density is achieved. This crucible is placed in a cold furnace and heated to a sintering temperature of 785°C in air, followed by furnace cooling. No significant deviations in the properties of the foams have been noted for sintering times ranging from a few hours to 144 h. The temperature of the furnace is controlled to within ±5°C over a length of 120 mm, such that homogenous preforms with a length of about 100 mm and a diameter up to 38 mm can be produced (Marchi C. San, 2001).

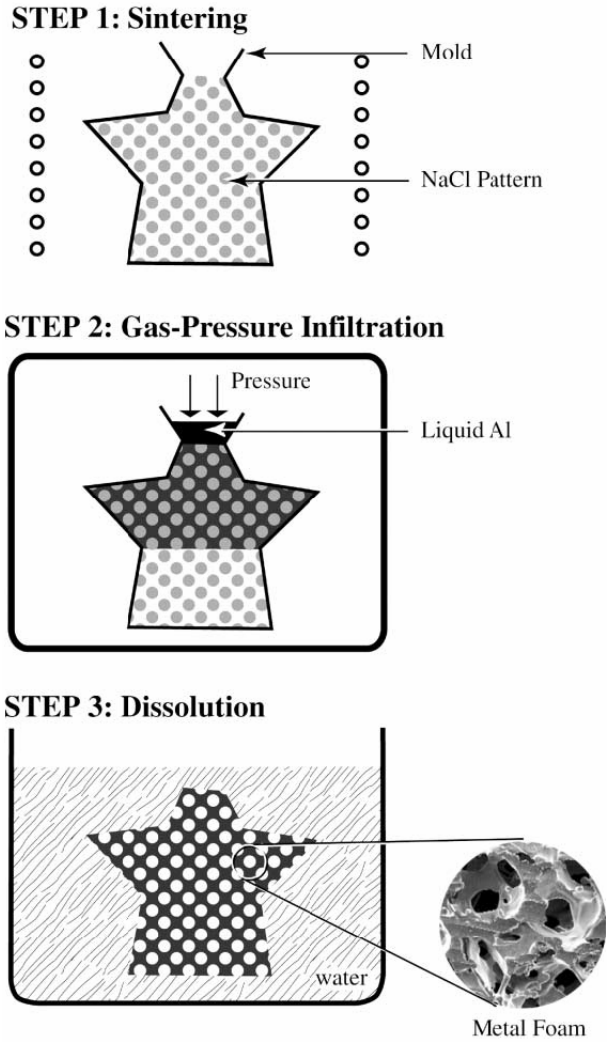

Figure 2. Schematic of the replication process for the production of metallic foam.

After sintering, the salt pattern is removed, inserted into a similar alumina crucible coated with graphite, and a billet of aluminum is placed on top of the pattern. This assembly is placed in a hot-wall gas-pressure infiltration apparatus, where it is heated to 750°C under vacuum. Once the temperature has stabilized, the system is pressurized with argon to a pressure of 0.5 MPa, such that the liquid aluminum infiltrates the preform. After infiltration is complete, directional solidification is initiated from the bottom of the crucible upwards by lowering the crucible onto a cold copper chill within the infiltration apparatus. After solidification, the material is removed from the infiltration apparatus and machined to the desired dimensions prior to removal of the salt. The salt is subsequently leached by submersion in distilled water (Marchi C. San, 2001).

3. FOAM MODEL

The method creating foams just like processing of foams. So, metallic foams are regarded as discontinuous medium and pores of different size and position, fitted to uniform distribution and filled with void, are created in the metal to model the real geometry. Naturally material parameters needed for metallic foams are just those of original metal material, which have been developed extensively and successfully.

Further more, the geometry of foams is too complex to be created by finite element method. However, it is very easy for SPH method, because it can arrange particles arbitrarily (Fig. 3). For nonhomogeneity of foams, numerical simulations have to be 3-dimentional.

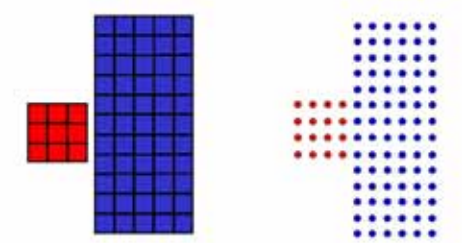

Figure 3. Left: Grids of Language; Right: Particles of SPH.

The mean radius of spheres

$$\bar{r} = d / \alpha \qquad (1)$$

where d is the mean diameter of pores and α is a factor to change the density of foams, usually $0<\alpha<1$. The radius of a sphere

$$r = f(\bar{r}) \qquad (2)$$

where f is a distribution function. The coordinate

$$x_i = (n-1)d + g(0.5d) + \Delta x_i \qquad (3)$$

where n is the sequence number of pore, g is a distribution function and applied to adjust the relative position of spheres in a row, Δx_i is a *0-d* stochastic value and applied to adjust the position of spheres of every row. A schematic of position of spheres on the material boundary is shown in Fig. 4 and in the material is shown in Fig. 5.

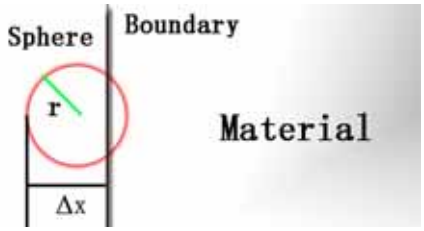

Figure 4. Schematic of a sphere on the boundary of foams.

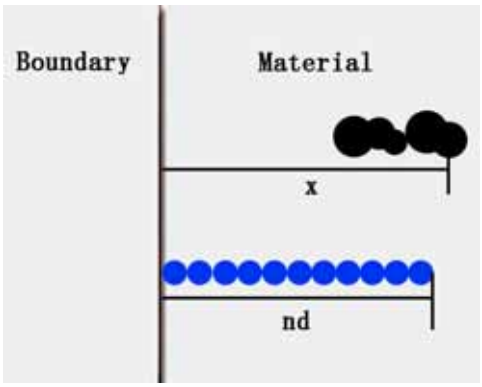

Figure 5. Schematic of spheres in the foam.

Such an SPH program with the foam model is developed. The foam created is shown in Fig. 6.

Figure 6. An open-cell foam, whose weight is 9.2% the weight of solid Aluminum, is created by the program, and showed as SPH particles.

4. THEORETICAL FUNDAMENTALS

The foundation of SPH is interpolation theory. The conservation laws of continuum dynamics, in the form of partial differential equations, are transformed into integral equations through the use of an interpolation function that gives the 'kernel estimate' of the field variables at a point. Computationally, information is known only at discrete points, so that the integrals are evaluated as sums over neighboring particles (Randles P.W., 1996).

The conservation equations of continuum mechanics are

$$\frac{d\rho}{dt} = -\rho \nabla \cdot v \qquad (4)$$

$$\frac{dv}{dt} = \frac{\nabla \sigma}{\rho} \qquad (5)$$

$$\frac{de}{dt} = \frac{\sigma \nabla \cdot v}{\rho} \qquad (6)$$

The transformation of Eq. 4-6 into particle equations yields the following set of SPH Eq. 7-9

$$\frac{d\rho_i}{dt} = \rho_i \sum_j \frac{m_j}{\rho_j} \left(u_i^\beta - u_j^\beta\right) W_{ij,\beta} \qquad (7)$$

$$\frac{du_i^\alpha}{dt} = \sum_j m_j \left(\frac{\sigma_i^{\alpha\beta}}{\rho_i^2} + \frac{\sigma_j^{\alpha\beta}}{\rho_j^2} - \Pi_{ij} \right) W_{ij,\beta} \qquad (8)$$

$$\frac{de_i}{dt} = \frac{1}{2} \sum_j m_j \left(u_j^\beta - u_i^\beta\right) \left(\frac{\sigma_i^{\alpha\beta}}{\rho_i^2} + \frac{\sigma_j^{\alpha\beta}}{\rho_j^2} - \Pi_{ij} \right) W_{ij,\beta} \qquad (9)$$

Where ρ_i, m_i, u_i^α and e_i are the density, mass, velocity, stress and specific internal energy of ith particle, respectively, and $W_{ij,\beta}$ is the derivative of the kernel function W_{ij}.

The artificial viscous pressure Π_{ij} traditionally used has been the Monaghan-Gingold form

$$\Pi_{ij} = \begin{cases} \dfrac{-\alpha \bar{c}_{ij} \mu_{ij} + \beta \mu_{ij}^2}{\overline{\rho_{ij}}}, & v_{ij} \cdot x_{ij} < 0 \\ 0, & v_{ij} \cdot x_{ij} \geq 0 \end{cases} \qquad (10)$$

where

$$\mu_{ij} = \frac{h_{ij} v_{ij} \cdot x_{ij}}{|x_{ij}|^2 + \eta h_{ij}^2}, \bar{c}_{ij} = \frac{1}{2}(c_i + c_j),$$
$$\bar{\rho}_{ij} = \frac{1}{2}(\rho_i + \rho_j), v_{ij} = v_i - v_j, h_{ij} = \frac{1}{2}(h_i + h_j) \quad (11)$$

Here, the parameters α and β are of order unity and ε is usually taken as 0.1. The sound speed on particle *i* is denoted by c_i.

The interpolation kernel or smoothing function most widely used in SPH is the B-spline

$$W_{ij}(S,h) = \alpha_d \begin{cases} \frac{2}{3} - S^2 + \frac{1}{2}S^3, & 0 \le S < 1 \\ \frac{1}{6}(2-S)^3, & 1 \le S < 2 \\ 0, & S \ge 2 \end{cases} \quad (12)$$

where $S = |x - x'|/h$, and α_d is given by $\alpha_d = 3/2\pi h^3$ for the 3-dimensitional problem.

5. VALIDATION

As numerical simulations by means of the foam model, the HVI responses of an Al projectile striking to a structure of double bumper shield are simulated and the results are shown in graphs and compared with experiments.

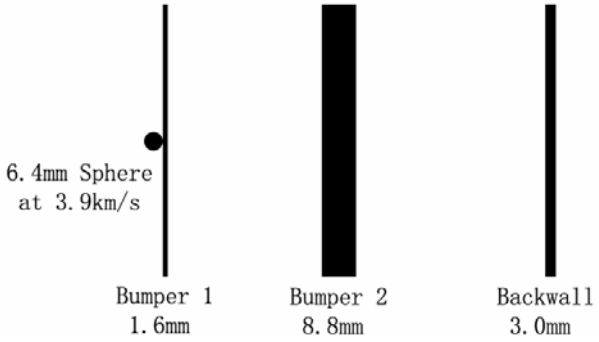

Figure 7. Schematic of configuration.

The geometry consists of a 6.4mm diameter sphere with an initial velocity of 3.9km/s impacting normally onto a 1.6mm thick bumper plate. A second bumper plate, of thickness 8.8mm, was placed 136mm behind the rear face of the first bumper plate. A backwall, consisting of a 3.0mm thick layer was placed 151mm behind the rear face of the second bumper plate. A schematic of this configuration is shown in Fig. 7. The bumper 1 and backwall are made of Al2024, the bumper 2 is open-cell Al2024 foam, whose mean pore size is 0.6mm and whose weight is 43% the weight of solid Aluminum, and the projectile is Al2017. The structure was modeled using an SPH method with a constant smoothing length of 0.2mm.

Fig. 8 shows geometry of bumper 1 after impact with experiment and simulation. The bumper 1 was penetrated by the projectile, with an average final hole diameter of 11.3mm of experiment and 11.5mm of simulation.

Fig. 9 shows geometry of bumper 2 after impact with experiment and simulation. The bumper 2 was just penetrated by debris clouds. There are a lot of ringed craters on the foam.

There wasn't any damage on the backwall, for the bumper 2 absorbed almost all the energy of debris clouds.

Fig. 8 and Fig. 9 show good agreement of both the experiment and numerical simulation.

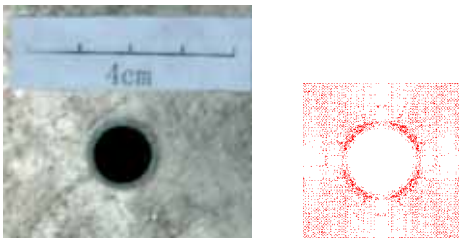

Figure 8. Bumper 1, after impact. Left: experiment; right: simulation.

Figure 9. Bumper 2, after impact. Left: experiment; right: simulation.

6. BEHAVIOR OF AL-FOAMS

The behavior variation of open-cell Al-foams under hypervelocity impact was investigated by numerical simulation with respect to relative density, which is the ratio of density of foams to that of base metal, and pore size as well as pore size homogeneity.

A Whipple structure of foam bumper and Al backwall is used. The geometry consists of a 3.0mm diameter sphere with an initial velocity of 6.3km/s impacting

normally onto foam bumper plate. A backwall, consisting of a 1.5mm thick layer was placed 100mm behind the front face of the bumper plate. The backwall is made of Al2024, the bumper is open-cell Al2024 foam and the projectile is Al1100.

Fig. 10 shows the comparison of different pore size of foams used in the numerical simulation. It is seen from the figure that crater depth of backwall turns lower, then higher, varied with pore size. But Fig. 10 doesn't mean the rule of shielding performance of Al-foams varied with pore size because of stochastic geometry of foams.

That crater depth varies with relative density and homogeneity is also simulated. The results don't hint any trend.

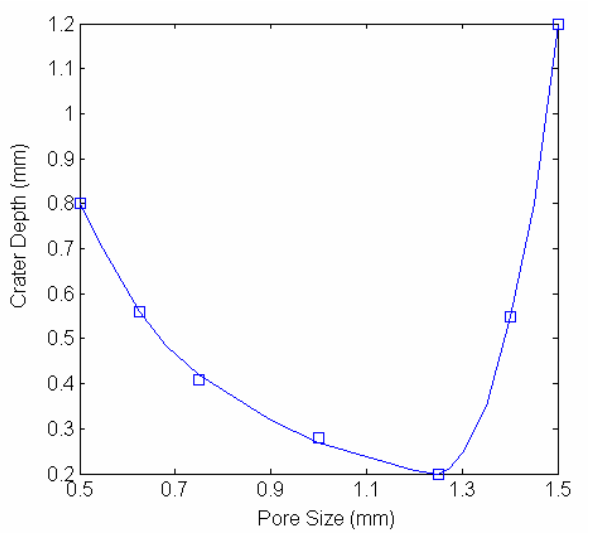

Figure 10. Comparison of different pore size.

7. CONCLUSIONS

A new foam model is suggested to simulate hypervelocity impact problems with foams. The course of creating the model just likes processing foams and the model is easy to be created with SPH method. To validate the model, a numerical simulation of normal impact incidence was carried out and compared with test data. Good agreement was obtained.

Behavior of open-cell Al-foams was investigated and the results showed that the behavior is complex and a lot of tests and simulations have to be carried out to obtain the rules.

REFERENCES

Randles P.W., Libersky L.D., Smoothed Particle Hydrodynamics: Some recent improvements and applications, *Computer Methods in Applied Mechanics and Engineering*, Vol. 139, 375-408, 1996.

Marchi C. San and Mortensen A., Deformation of Open-cell Aluminum Foam, *Acta Materialia*, Vol. 49, 3959–3969, 2001

John Banhart, Manufacture, Characterisation and Application of Cellular Metals and Metal foams, *Progress in Materials Science*, Vol. 46, 559–632, 2001

Thoma K., Schafer F., Hiermaier S., Scheider E., An Approach to Achieve Progress in Spacecraft shielding, *Advances in Space Research*, Vol. 34, 1063-1075, 2004.

Hans-Peter Degischer and Brigitte Kriszt, *Handbook of Cellular Metals: Production, Processing, Applications*, Wiley-VCH Verlag GmbH, 2002.

Marchi C. San., Despois, J. F. and Mortensen, A., *Metal Matrix Composites and Metallic Foams*, Euromat 99, Proc. Conf., Munich, ed. T. W. Clyne and F. Simancik. DGM/Wiley-VCH, 1999